



## Short communication

## Novel agmatine and agmatine-like peptidomimetic inhibitors of the West Nile virus NS2B/NS3 serine protease

Huichang Annie Lim, Joma Joy, Jeffrey Hill, Cheng San Brian Chia\*

*Experimental Therapeutics Centre, Agency for Science, Technology and Research (A\*STAR), 31 Biopolis Way, Nanos #03-01, Singapore 138669, Singapore*

## ARTICLE INFO

## Article history:

Received 16 February 2011

Received in revised form

5 April 2011

Accepted 20 April 2011

Available online 28 April 2011

## Keywords:

Agmatine

Arginine mimetic

Serine protease inhibitor

West Nile virus

## ABSTRACT

This communication reports the synthesis and inhibitory activities of novel non-covalent peptidomimetic inhibitors of the West Nile virus NS2B/NS3 protease containing a decarboxylated P1 arginine (agmatine; 4-aminobutylguanidine) and related analogues. One agmatine peptidomimetic (4-phenylphenacetyl-Lys-Lys-agmatine; compound **2**) was shown to be a competitive inhibitor with a binding affinity of  $K_i$   $2.05 \pm 0.13 \mu\text{M}$  and was inactive against thrombin ( $\text{IC}_{50} > 100 \mu\text{M}$ ). Our results suggest that peptidomimetics with agmatine at the P1 position could potentially be employed as starting tools in the design of non-covalent competitive protease inhibitors due to their relative stability and ease of chemical synthesis compared to inhibitors containing reactive electrophilic warheads.

© 2011 Elsevier Masson SAS. All rights reserved.

## 1. Introduction

The West Nile virus (WNV) is a mosquito-borne virus of the Flaviviridae family. Originating from Africa, it has spread to humans in different continents, including North America [1,2]. Between 1999 and 2009, the United States Center for Disease Control reported more than 20,000 people in the United States have been infected, resulting in 1163 fatalities [3]. Symptoms of infection include fever, headaches, chills, diaphoresis and lymphadenopathy which can lead to high fever known as the 'West Nile Fever'. Some of these cases progress to meningitis, coma and death [4].

The WNV has a single-strand, positive-sense, 11-kb RNA genome which serves as a messenger RNA for protein synthesis as well as a template for RNA replication in a mammalian host cell. The viral genome encodes seven nonstructural proteins (NS1, NS2A, NS2B, NS3, NS4A, NS4B and NS5) [5] and one attractive target for antiviral drug development is NS3 [6–8]. In the cytoplasm of a host cell, NS3 complexes to its NS2B cofactor to form a functional trypsin-like serine protease which cleaves polyprotein precursors into mature viral proteins [9]. The NS2B/NS3 complex recognizes and selectively cleaves the C-terminal end of two consecutive, highly-conserved basic residues (Fig. 1) [10]. This unusual specificity is not shared by many mammalian proteases and could thus be exploited as an antiviral drug target [6,11].

A common strategy used for the inhibition of the NS2B/NS3 protease involved covalent inhibitors that compete with the substrate for the catalytic site. Such peptide-based covalent inhibitors have their C-terminal carboxyl group chemically modified into reactive electrophilic 'warheads' (see [11,12] for reviews). A popular warhead is the aldehyde functional group and peptide aldehydes have been shown to inhibit the WNV NS2B/NS3 protease at sub-micromolar potencies [13]. However, warhead peptidomimetics have several undesirable characteristics, including lack of selectivity over other trypsin-like proteases due to their high reactivity and low chemical stability, curtailing their potential for drug development [14]. In this report, we investigated if peptidomimetics without electrophilic warheads could inhibit the WNV NS2B/NS3 protease. These inhibitors do not bind covalently to the catalytic serine in the active site but instead employ hydrophobic and/or electrostatic interactions to compete with the natural substrate for the active site. Such inhibitors should be less reactive and hence more 'druggable' compared to warhead inhibitors.

Our strategy focused on peptidomimetics containing a P1 decarboxylated arginine (agmatine; 4-aminobutylguanidine) and structurally-related analogues. Agmatine-containing peptidomimetics have been reported to inhibit trypsin-like serine proteases like furin, a mammalian protease responsible for the cleavage of inactive protein precursors involved in many physiological pathways [14] and thrombin, a protease involved in blood-clotting [15,16]. These inhibitors contained agmatine and agmatine analogues at the P1 position and were found to be competitive inhibitors with micromolar to sub-micromolar potencies. On this

\* Corresponding author. Tel.: +65 64070348; fax: +65 64788768.

E-mail address: [cschia@etc.a-star.edu.sg](mailto:cschia@etc.a-star.edu.sg) (C. San Brian Chia).

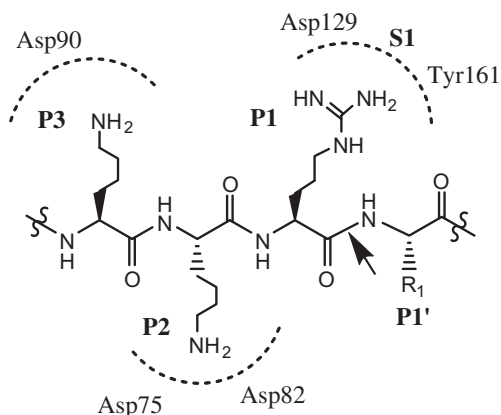


**Fig. 1.** Schematic diagram of a peptide substrate showing the position of the scissile bond (arrowed) and the basic residues: Lys (P3, P2) and Arg (P1). The WNV protease residues in the S1–S3 binding sites participating in substrate binding are numbered based on the crystal structure 3E90.pdb.

basis, we designed and synthesized ten novel compounds incorporating agmatine and its analogues at the P1 position of the WNV peptide substrate recognition sequence: Lys(P3)-Lys(P2)-Arg(P1) and tested them for inhibitory activities against WNV NS2B/NS3 serine protease (Fig. 2).

Lastly, we explored the enzyme inhibitory activity of our two most potent inhibitors against thrombin to gain an insight into their selectivity against trypsin-like serine proteases.

## 2. Results and discussion

### 2.1. Chemistry

The general synthetic procedure for compounds **1–10** is shown in Scheme 1: the appropriate diamine was guanylated with *N,N*-di(*t*-butoxycarbonyl)-*S*-methylisothiourea based on the method by Verdini et al. [17] to give the Boc-protected agmatine and its analogues. These were then coupled with Fmoc-Lys(Boc)-Lys(Boc)-OH using *O*-benzotriazole-*N,N,N',N'*-tetramethyluroniumhexafluorophosphate (HBTU) as coupling reagent. After Fmoc removal by 1,8-diazabicyclo[5.4.0] undec-7-ene (DBU), the deprotected peptidomimetics were *N*-capped with acetic anhydride or 4-biphenylacetic acid. Finally, the Boc protecting groups were removed by TFA treatment and the pseudo-peptides were purified (HPLC) and characterized (LCMS).

### 2.2. Biological activity

Compound **1** showed an inhibitory activity of  $IC_{50} = 18.2 \pm 4.2 \mu\text{M}$  against WNV NS2B/NS3 protease (Table 1), proving that

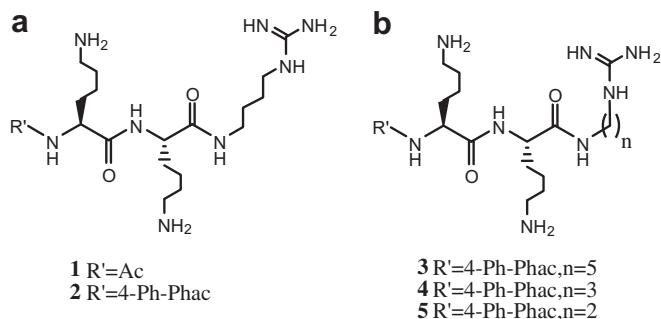


**Fig. 2.** Structures of compounds (a) **1** and **2**; (b) **3–5**. Agmatine is shown in the hashed box. Structures of compounds **6–10** can be found in Table 1.

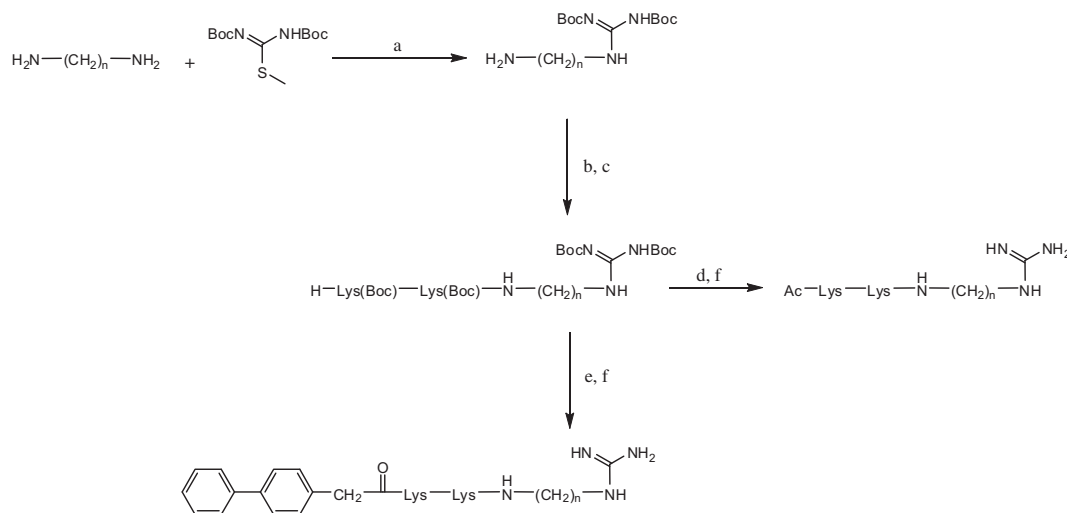
agmatine-containing peptidomimetics could inhibit the WNV NS2B/NS3 serine protease.

Encouraged by this, we synthesized compound **2** where the *N*-terminus was capped with a 4-phenyl-phenacetyl (4-Ph-Phac) group. This group has been reported to be the most potent *N*-capping group in a panel of tripeptide aldehyde WNV inhibitors ( $IC_{50} = 32 \text{ nM}$  for 4-Ph-Phac-KKR-H) and computer docking studies using simulated annealing showed that the 4-Ph-Phac group could squeeze into the S4 WNV protease binding site [13]. Expectedly, the potency of **2** improved approximately 4-fold compared with **1**, with an  $IC_{50}$  of  $4.7 \pm 1.2 \mu\text{M}$  (Table 1). A Lineweaver–Burk plot of inhibitor **2** showed that it acted as a competitive inhibitor with a  $K_i$  of  $2.05 \pm 0.13 \mu\text{M}$  (Fig. 3).

We next tested a panel of compounds containing agmatine homologues with different alkyl chain lengths (compounds **3–5**). Using the recent crystal structure of the tripeptide aldehyde inhibitor Naphthoyl-KKR-H complexed to WNV NS2B/NS3 protease (3E90 pdb [18];), the P1 arginine's guanidino group was observed to take part in electrostatic attraction with the side-chain carboxylate anion of Asp129 of NS3 within a distance of 3.2–4.3 Å in the S1 binding site. Altering the length of the agmatine alkyl chain should alter the guanidino-carboxylate distance and affect binding affinity. As expected, compounds **3–5** failed to inhibit the NS2B/NS3 enzyme ( $IC_{50} > 100 \mu\text{M}$ ; Table 1). An intriguing observation was that the addition or removal of just one methylene group (compounds **3** and **4** respectively) abrogated all binding affinity, suggesting that a 4-carbon alkyl chain between the amide and guanidino group was optimal for binding. Indeed, molecular modelling of compound **3** using 3E90 pdb as a template showed that lengthening the alkyl chain by one carbon caused the guanidino group of **3** to clash with Asp129 side-chain. Removing one methylene from the alkyl chain (compound **4**) increased the distance between the guanidino group and the carboxyl side-chain of Asp129 to approximately 4.1–5.0 Å, possibly disrupting the salt bridge between them. With this knowledge, we synthesized compound **6** in which the presence of a *trans*-( $\beta$ - $\gamma$ ) double bond rigidifies the 4-carbon alkyl chain. Interestingly, the unsaturated analogue **6** was approximately 13-fold less potent than its saturated counterpart **2** ( $IC_{50}$  61.2  $\pm$  8.6 and 4.7  $\pm$  1.2  $\mu\text{M}$  respectively), suggesting that a flexible 4-carbon alkyl chain was needed for optimal positioning of the guanidino group relative to Asp129 and Tyr161 in the S1 binding site. Based on these results, we could conclude that a saturated 4-carbon chain was needed for optimal binding.

A final series of inhibitors containing conformationally restrained agmatine analogues **7–10** (Table 1) were synthesized using inhibitor **2** as a template to test the effect of increasing the agmatine *n*-butyl chain rigidity on enzyme S1 site binding affinity. Hence, 5 and 6-membered cyclic agmatine mimetics **7–10** were synthesized and assayed. Experimental results revealed that 6-membered analogues **7** and **8** did not possess any inhibitory activities ( $IC_{50} > 100 \mu\text{M}$ ), suggesting that the rigid 6-membered rings may have oriented the guanidino group away from its optimal position in the S1 binding site. This was supported by molecular modelling studies using the crystal structure 3E90 pdb adopted by the tripeptide aldehyde inhibitor KKR-H when complexed to the WNV protease. Our models revealed that replacing the flexible agmatine *n*-butyl chain in compound **2** with 6-membered rings steered the guanidino group away from the S1 binding site which possibly abrogated all binding affinities (Fig. 4A and B).

The assay results for agmatine mimetics containing 5-membered pyrrolidine rings (compounds **9** and **10**) were more interesting; compound **9** showed no inhibitory activity ( $IC_{50} > 100 \mu\text{M}$ ) while **10** exhibited moderate activity ( $IC_{50}$  20.0  $\pm$  5.8  $\mu\text{M}$ ). Our molecular models suggested that the stereogenic carbon in the pyrrolidine ring played an important role in orienting the guanidino group either



**Scheme 1.** (a) DIPEA, DCM, 25 °C, 16 h; (b) Fmoc-Lys(Boc)-Lys(Boc)-OH, HBTU, DIPEA, DMF, 25 °C, 1 h; (c) DCM, DBU, 25 °C, 1 h; (d) acetic anhydride, DIPEA, DMF, 25 °C, 30 min; (e) 4-biphenylacetic acid, HBTU, DIPEA, DMF, 25 °C, 1 h; (f) TFA, DCM, 25 °C, 30 min.

**Table 1**  
Inhibitory data of WNV peptidomimetic inhibitors with the general sequence: P4-Lys-Lys-P1. Greek symbols illustrate the relative position of the guanidino  $\epsilon$ -nitrogen in relation to the amide nitrogen.

Compound	P4	P1	IC <sub>50</sub> ( $\mu$ M)
1	Acetyl		18.2 $\pm$ 4.2
2	4-Ph-Phac		4.7 $\pm$ 1.2
3	4-Ph-Phac		>100
4	4-Ph-Phac		>100
5	4-Ph-Phac		>100
6	4-Ph-Phac		61.2 $\pm$ 8.6
7	4-Ph-Phac		>100
8	4-Ph-Phac		>100
9	4-Ph-Phac		>100
10	4-Ph-Phac		20.0 $\pm$ 5.8

away or towards the S1 binding site (Fig. 4C and D respectively). The molecular model of compound **10** showed the guanidino group orienting towards the S1 binding site (Fig. 4D) and was 4-fold less potent than inhibitor **2** (IC<sub>50</sub> 20.0  $\pm$  5.8 and 4.7  $\pm$  1.2  $\mu$ M respectively). A plausible reason could be that the guanidino group of inhibitor **10** may not be in an optimal position compared to inhibitor **2**. Another reason could be the loss of one H-bond interaction between **10** and the protease. In fact, by superimposing **10** to the 3E90 pdb crystal structure, it was observed that the P1 arginine amide proton was involved in H-bonding to Gly151 carbonyl oxygen of the NS3 protease. The removal of the amide proton with a pyrrolidine ring substitution would result in one less H-bonding interaction between **10** and the protease (Fig. 5), reducing its binding affinity.

Overall, our experimental results suggested that the WNV NS2B/NS3 S1 binding site was highly selective for a P1 agmatine. Substituting 5- or 6-membered rings into the carbon chain severely abrogated the inhibitory activities of our test compounds.

Finally, we assayed the two most potent inhibitors **1** and **2** against thrombin, a mammalian serine protease involved in blood-clotting that is selective for peptide substrates with a P1 Arg. Experimental results showed that both did not inhibit thrombin at a concentration of 100  $\mu$ M, suggesting that the P2 and P3 Lys may not fit in the thrombin S2 and S3 binding sites respectively, resulting in selectivity towards the WNV NS2B/NS3 protease.

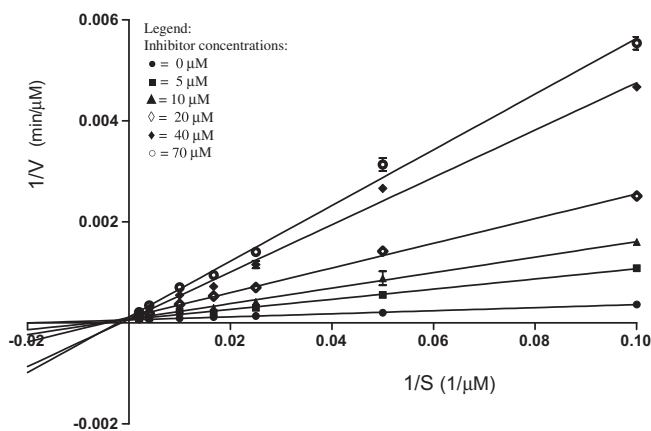


**Fig. 3.** Lineweaver-Burk plot for the inhibition of the WNV NS2B/NS3 protease by inhibitor **2** using Pyr-RTKR-AMC as substrate.

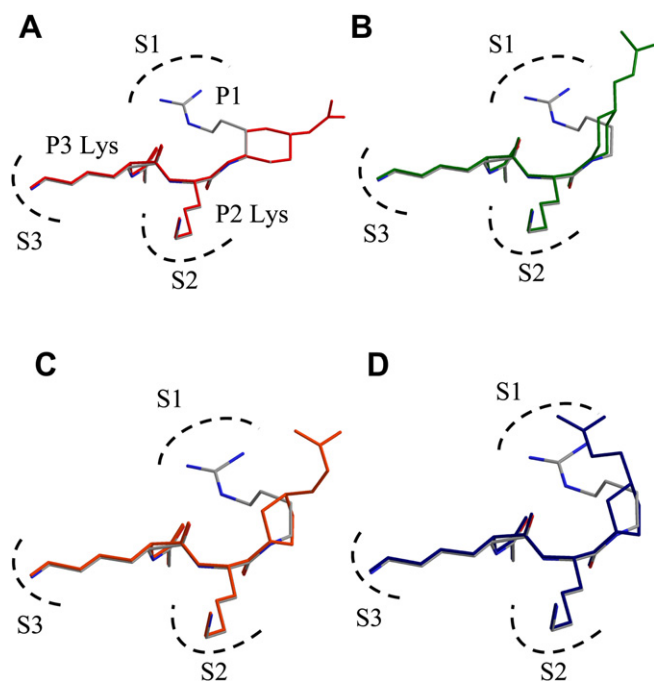


**Fig. 4.** Stick-models of compound **2** (grey) superimposed on compounds: (A) **7** (red); (B) **8** (green); (C) **9** (orange) and (D) **10** (blue) using the crystal structure 3E90 pdb as a template. The NS2B/NS3 protease and 4-Ph-Phac N-cap have been omitted for clarity. (For interpretation of the references to colour in this figure legend, the reader is referred to the web version of this article.)

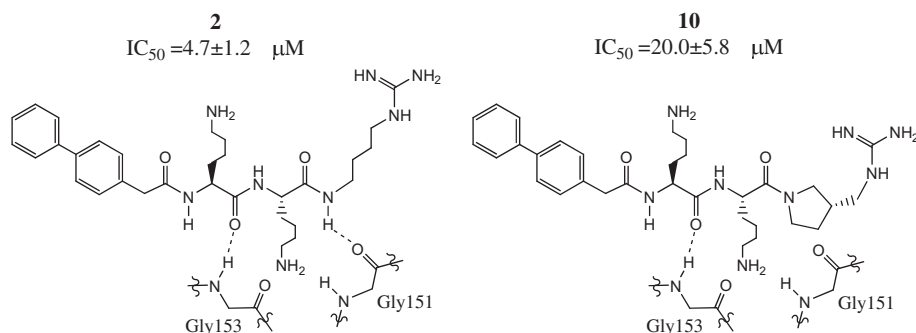


**Fig. 5.** Schematic diagrams of inhibitors **2** and **10** showing H-bonding interactions to Gly151 and Gly153 of WNV NS2B/NS3 protease. Hashed lines represent H-bonds. The loss of one H-bond in **10** may explain the decrease in inhibitory activity. Residue numbers are based on the crystal structure 3E90 pdb. Only Gly151 and Gly153 of the protease are shown for simplicity.

### 3. Conclusion

Our results suggested that the S1 binding site of the WNV NS2B/NS3 protease was highly specific for P1 agmatine and would not accommodate homologues, 5 and 6-membered alkyl rings. Due to the lack of a reactive warhead and a chiral  $\alpha$ -carbon at the P1 position, the synthesis of agmatine-containing peptidomimetics was less complex than their electrophilic-warhead counterparts. Hence, agmatine peptidomimetics could serve as a convenient starting point to explore the chemistry of the P1 residue of trypsin-like protease inhibitors, including viral and mammalian protease inhibitors. We also postulate that decarboxylated P1 peptidomimetics can potentially be employed in the design of novel competitive inhibitors against other proteases like aspartyl, cysteine, threonine and metalloproteases.

## 4. Experimental protocols

### 4.1. Chemistry

All reagents and solvents were obtained from commercial sources and were used without further purification. Acetonitrile was purchased from Merck KGaA (Germany). Fmoc-Lys(Boc)-Lys(Boc)-OH was purchased from GL Biochem (China). Deuterated solvents were purchased from Cambridge Isotope Laboratories (USA). All other reagents were purchased from Sigma–Aldrich (USA). Flash chromatography was performed on an automated system (Teledyne Isco Combiflash RF200) using a silica column (RediSep RF, 230–400 Mesh, 60 Å average pore size). Crude target inhibitors were purified using a reverse-phase C18 column (Waters X-bridge) on a high performance liquid chromatography (HPLC) system with an ultraviolet detector set at 215 nm (Shimadzu Prominence). The mobile phase consisted of solvent A (water) and solvent B (acetonitrile). The gradient started with 1% solvent B for 5 min which was increased to 11% in 40 min. All target compounds were characterized by electrospray ionization–time of flight–mass spectrometry (ESI-TOF-MS; Agilent 6224 TOF using Mass Hunter software). NMR spectra were recorded on a Bruker spectrometer (400 MHz) in CD<sub>3</sub>OD. Chemical shifts were expressed as  $\delta$  (ppm) relative to the solvent peak.

#### 4.1.1. Synthesis of compounds 1–10

The detailed synthetic procedures for compounds **1**, **3**–**10** are reported in the supplementary notes. The synthetic procedure for the most potent inhibitor (compound **2**) is described herein:

1,4-Diaminobutane (0.5 mmol, 44 mg), *N,N*-di-(*t*-butoxycarbonyl)-*S*-methylisothiourea (0.4 mmol, 116 mg) and *N,N*-diisopropylethylamine (DIPEA; 1 mmol, 175  $\mu$ L) were dissolved in anhydrous CH<sub>2</sub>Cl<sub>2</sub> (6 mL). The mixture was stirred at 25 °C, 16 h under N<sub>2</sub> atmosphere and the resulting guanylated amine was purified by flash chromatography using a CH<sub>2</sub>Cl<sub>2</sub>/methanol gradient and monitored using MS. The solvent was removed *in vacuo* to give a colourless oil (79 mg, 0.24 mmol, 60%). Fmoc-Lys(Boc)-Lys(Boc)-OH (0.264 mmol, 184 mg), HBTU (0.48 mmol, 182 mg), DIPEA (0.72 mmol, 122  $\mu$ L) and dimethylformamide (DMF, 10 mL) were added to the oil (79 mg, 0.24 mmol) and the mixture was stirred at 25 °C for 1 h. The contents were dissolved in ethyl acetate (30 mL) and washed with brine (50 mL) thrice. The organic phase was removed *in vacuo* to give a cloudy gel which was dissolved in CH<sub>2</sub>Cl<sub>2</sub> (10 mL). DBU (0.36 mmol, 54  $\mu$ L) was added to the mixture

and stirred at 25 °C for 1 h. The resulting dipeptide was purified by flash chromatography using a CH<sub>2</sub>Cl<sub>2</sub>/methanol gradient monitored using MS. The solvent was removed *in vacuo* to give a colourless oil (157 mg, 0.20 mmol, 83%). 2-(biphenyl-4-yl)acetic acid (0.22 mmol, 43 mg), HBTU (0.44 mmol, 167 mg), DIPEA (0.66 mmol, 113 μL) and DMF (10 mL) were added to the oil and the mixture was stirred at 25 °C, 30 min. The contents were dissolved in ethyl acetate (30 mL) and washed with brine (50 mL) thrice. The organic phase was removed *in vacuo* to give a cloudy gel. The resulting N-capped dipeptide was purified by flash chromatography using a CH<sub>2</sub>Cl<sub>2</sub>/methanol gradient and monitored at 254 nm. The solvent was removed *in vacuo* to give a colourless oil (141 mg, 0.144 mmol, 72%) before being dissolved in CH<sub>2</sub>Cl<sub>2</sub> (1 mL) and stirred with TFA (1 mL) at 25 °C, 30 min. The mixture was dried under a N<sub>2</sub> stream, re-dissolved in methanol (1 mL) and purified by HPLC (water and acetonitrile solvent) to give the target product (51 mg, 0.088 mmol, 61%). Spectral data: <sup>1</sup>H NMR (400 MHz, CD<sub>3</sub>OD) δ 1.29–1.96 (16H, m), 2.82–3.23 (8H, m), 3.64 (2H, s, Ar–CH<sub>2</sub>–CO–), 4.21–4.31 (2H, m, α-Hs), 7.30–7.62 (9H, m, aromatics); <sup>13</sup>C NMR (100 MHz, CD<sub>3</sub>OD) δ 22.4, 22.5, 25.7, 26.0, 26.5, 26.7, 28.1, 30.0, 30.5, 38.4, 39.1, 40.7, 41.6, 53.1, 53.9, 126.4, 126.8, 127.1, 128.6, 129.4, 134.5, 139.8, 140.5, 157.3, 172.7, 173.0, 173.2. ESI-TOF-MS: *m/z* calc C<sub>31</sub>H<sub>49</sub>N<sub>8</sub>O<sub>3</sub> (M + H<sup>+</sup>) 581.3922, found 581.3918.

## 4.2. Biological activities

### 4.2.1. WNV NS2B/NS3 enzyme inhibition assay

WNV NS2B/NS3 inhibitory assays were based on published work [10] and performed in a buffer at pH 8.0 containing Tris–HCl (10 mM), CHAPS (1 mM) and glycerol (20% v/v). The enzyme (20 nM) and varying concentrations of inhibitor were next added and pre-incubated at 25 °C for 1 h. The reaction was initiated by the addition of the fluorogenic peptide substrate Pyr-RTKR-AMC (Bachem, Switzerland) to make a final concentration of 20 μM. The reaction components were shaken for 5 s and the reaction progress monitored at 37 °C by measuring the increase in fluorescence (λ<sub>ex</sub>355 nm and λ<sub>em</sub>460 nm) every 45 s for 1 h on a SpectraMax Gemini XS plate reader (USA). Experiments were done in duplicates. IC<sub>50</sub> values were derived by fitting the initial velocity against the log [inhibitor] with a sigmoidal dose response curve using GraphPad Prism 5 software. Nona-D-Arg-NH<sub>2</sub> peptide (GenScript, USA) was used as positive control.

### 4.2.2. Kinetic measurements for K<sub>i</sub> determination

The most potent inhibitor (compound **2**) was incubated at various concentrations (0, 5, 10, 20, 40 and 70 μM) at pH 8.0 with WNV NS2B/NS3 protease (20 nM), Tris–HCl (10 mM), CHAPS (1 mM) and glycerol (20% v/v) at 25 °C for 1 h. Next, the substrate Pyr-RTKR-AMC (Bachem, Switzerland) was added at different concentrations (10, 20, 40, 60, 100, 250 and 500 μM) and the reaction components shaken for 5 s. The rate of substrate hydrolysis was monitored at 37 °C by measuring the increase in fluorescence (λ<sub>ex</sub>355 nm and λ<sub>em</sub>460 nm) every 45 s for 1 h on a SpectraMax Gemini XS plate reader (USA). The Lineweaver-Burk plot was generated by plotting the reciprocal of hydrolysis rate (1/V) against the reciprocal of substrate concentration (1/S) at various inhibitor concentrations. The K<sub>i</sub> for inhibitor **2** was derived by non-linear

regression fit by selecting the competitive inhibition model in GraphPad Prism 5 software.

### 4.2.3. Thrombin inhibition assay

The thrombin inhibitory assay was performed using the Anaspec Sensolyte AFC thrombin assay kit (USA). Thrombin (40 nM) and the inhibitor (100 μM) was incubated in a reaction buffer at 25 °C for 1 h before addition of the AFC thrombin substrate. The reaction was monitored at 25 °C by measuring fluorescence intensity (λ<sub>ex</sub>380 nm and λ<sub>em</sub>500 nm) every 45 s for 1 h on a SpectraMax Gemini XS plate reader. The thrombin inhibitor NAPAP (N-2-naphthylsulfonyl-glycyl-4-amidinophenylalanine-piperidine) was used as positive control.

## 4.3. Molecular modelling software

Molecular modelling and energy minimization were performed using Chem3D Ultra (v.10) software (ChembridgeSoft, USA).

## Acknowledgements

We thank A\*STAR Biomedical Research Council for financial support, Dr. Manfred Raida for mass spectrometry analysis, Dr. Thomas Keller and Dr. Michael Entzeroth for critical reading of the manuscript.

## Appendix. Supplementary material

Supplementary data associated with this article can be found, in the online version, at doi:10.1016/j.ejmech.2011.04.055.

## References

- [1] L.H. Gould, E. Fikrig, *J. Clin. Invest.* 113 (2004) 1102–1107.
- [2] L.D. Kramer, J. Li, P.-Y. Shi, *Lancet Neurol.* 6 (2007) 171–181.
- [3] [www.cdc.gov/ncidod/dvbid/westnile/index.htm](http://www.cdc.gov/ncidod/dvbid/westnile/index.htm).
- [4] L.R. Petersen, A.A. Marfin, *Ann. Intern. Med.* 137 (2002) 173–179.
- [5] S. Mukhopadhyay, R.J. Kuhn, M.G. Rossmann, *Nat. Rev. Microbiol.* 3 (2005) 13–22.
- [6] K.J. Chappell, M.J. Stoermer, D.P. Fairlie, P.R. Young, *J. Biol. Chem.* 281 (2006) 38448–38458.
- [7] J.E. Knox, N.L. Ma, Z. Yin, S.J. Patel, W.-L. Wang, W.-L. Chan, K.R.R. Rao, G. Wang, X. Ngew, V. Patel, D. Beer, S.P. Lim, S.G. Vasudevan, T.H. Keller, *J. Med. Chem.* 49 (2006) 6585–6590.
- [8] C.G. Noble, Y.-L. Chen, H. Dong, F. Gu, S.P. Lim, W. Schul, Q.-Y. Wang, P.-Y. Shi, *Antivir. Res.* 85 (2010) 451–462.
- [9] C.E. Samuel, *Proc. Nat. Acad. Sci. USA* 99 (2002) 11555–11557.
- [10] T.A. Nall, K.J. Chappell, M.J. Stoermer, N.X. Fang, J.D. Tyndall, P.R. Young, D.P. Fairlie, *J. Biol. Chem.* 279 (2004) 48535–48542.
- [11] K.J. Chappell, M.J. Stoermer, D.P. Fairlie, P.R. Young, *Curr. Med. Chem.* 281 (2008) 2771–2784.
- [12] B. Walker, J.F. Lynas, *Cell. Mol. Life Sci.* 58 (2001) 596–624.
- [13] M.J. Stoermer, K.J. Chappell, S. Liebscher, C.M. Jensen, C.H. Gan, P.K. Gupta, W.-J. Xu, P.R. Young, D.P. Fairlie, *J. Med. Chem.* 51 (2008) 5714–5721.
- [14] G.L. Becker, F. Sielaff, M.E. Than, I. Lindberg, S. Routhier, R. Day, Y. Lu, W. Garten, T. Steinmetzer, *J. Med. Chem.* 53 (2010) 1067–1075.
- [15] D. Gustafsson, R. Bylund, T. Antonsson, I. Nilsson, J.-E. Nyström, U. Eriksson, U. Bredberg, A.-C. Teger-Nilsson, *Nat. Rev. Drug Discov.* 3 (2004) 649–659.
- [16] J. Wagner, J. Kallen, C. Ehrhardt, J.-P. Evenou, D. Wagner, *J. Med. Chem.* 41 (1998) 3664–3674.
- [17] A.S. Verdini, P. Lucietto, G. Fossati, C. Giordani, *Tetrahedron Lett.* 33 (1992) 6541–6542.
- [18] G. Robin, K. Chappell, M.J. Stoermer, S.-H. Hu, P.R. Young, D.P. Fairlie, J.L. Martin, *J. Mol. Biol.* 385 (2009) 1568–1577.